

Kaempferol and Its Glycoside Derivatives as Modulators of Etoposide Activity in HL-60 Cells

Magdalena Kluska

University of Łódź

Michał Juszczyk

University of Łódź

Jerzy Żuchowski

Institute of Soil Science and Plant Cultivation

Anna Stochmal

Institute of Soil Science and Plant Cultivation

Katarzyna Woźniak (✉ katarzyna.wozniak@biol.uni.lodz.pl)

University of Łódź

Research Article

Keywords: Kaempferol, Etoposide, DNA damage, Apoptosis, Cell cycle, Oxidative stress, HL-60 cells

Posted Date: January 7th, 2021

DOI: <https://doi.org/10.21203/rs.3.rs-138572/v1>

License:  This work is licensed under a Creative Commons Attribution 4.0 International License.

[Read Full License](#)

Kaempferol and its glycoside derivatives as modulators of etoposide activity in HL-60 cells

Magdalena Kluska ¹, Michał Juszcak ¹, Jerzy Żuchowski ², Anna Stochmal ², Katarzyna Woźniak ^{1*}

¹ University of Lodz, Faculty of Biology and Environmental Protection, Department of Molecular Genetics, 90-236 Lodz, Poland

² Department of Biochemistry and Crop Quality, Institute of Soil Science and Plant Cultivation, State Research Institute, 24-100 Pulawy, Poland

* Address for correspondence: Katarzyna Woźniak, Department of Molecular Genetics, Faculty of Biology and Environmental Protection, University of Lodz, Pomorska 141/143, 90-236 Lodz, Poland; Tel.: +48-42-635-47-76; Fax: +48-42-635-44-84; E-mail: katarzyna.wozniak@biol.uni.lodz.pl

Abstract

Kaempferol is a polyphenol found in a variety of plants. Kaempferol has antitumor properties by affecting proliferation and apoptosis of cancer cells. We investigated whether kaempferol and its glycoside derivatives: kaempferol 3-O-[(6-O-E-caffeoyl)- β -D-glucopyranosyl-(1 \rightarrow 2)]- β -D-galactopyranoside-7-O- β -D-glucopyranoside (P2), kaempferol 3-O-[(6-O-E-p-coumaroyl)- β -D-glucopyranosyl-(1 \rightarrow 2)]- β -D-galactopyranoside-7-O- β -D-glucopyranoside (P5) and kaempferol 3-O-[(6-O-E-feruloyl)- β -D-glucopyranosyl-(1 \rightarrow 2)]- β -D-galactopyranoside-7-O- β -D-glucopyranoside (P7) isolated from aerial parts of *Lens culinaris* Medik. affect the antitumor activity of etoposide in HL-60 cells. We analyzed the effect of kaempferol and its derivatives on cytotoxicity, DNA damage, apoptosis, cell cycle progression and free radicals induced by etoposide. We also studied the impact of kaempferol and its derivatives on the expression of *HO-1* and *Nrf-2* genes in HL-60 cells. We demonstrated that kaempferol increases the sensitivity of HL-60 cells to etoposide but does not affect apoptosis induced by this drug. Kaempferol also reduces the level of free radicals generated by etoposide. Unlike kaempferol, some of its derivatives reduce the apoptosis of HL-60 cells (P2 and P7) and increase the level of free radicals (P2 and P5) induced by etoposide. Our results indicate that kaempferol derivatives may have an opposite effect on the action of etoposide in HL-60 cells compared to kaempferol.

Keywords: Kaempferol; Etoposide, DNA damage; Apoptosis; Cell cycle; Oxidative stress; HL-60 cells

Abbreviations: DAPI – 4',6-diamidino-2-phenylindole; DMSO – dimethyl sulfoxide; *GAPDH* gene – glyceraldehyde-3-phosphate dehydrogenase gene; H₂O₂ – hydrogen peroxide; LMP agarose – low-melting-point agarose; NMP agarose – normal-melting-point agarose; PBS – phosphate-buffered saline

Introduction

Kaempferol [3,5,7-trihydroxy-2-(4-hydroxyphenyl)-4H-1-benzopyran-4-one] (Fig. 1A) is a flavonoid with anti-cancer potential that can be found in a variety of plants and plant-derived food products such as lentil, tea, broccoli or apples¹⁻³. Oxidative stress plays a major role in the development of many diseases, including cancer. It is suggested that the anticancer properties of phenolic compounds such as kaempferol are due to their antioxidant properties. Both kaempferol and its glycosides derivatives show antioxidant activity by scavenging free radicals as well as inhibiting pro-oxidant enzymes and activating antioxidant enzymes³.

The financial resources for health care increase all the time and cancer therapies are becoming more effective; however, leukemia is still characterized by high mortality and finding a cure for this disease is a real challenge for medicine. Chemotherapeutic agents used in leukemia treatment include topoisomerase II inhibitors, such as doxorubicin and etoposide. The efficiency of etoposide's cytostatic activity is dependent on the phase of the cell cycle and is highest in the S phase⁴. Unfortunately, standard chemotherapy is non-specific and affects both cancer and normal cells. Hence the need to look for compounds that could increase the antitumor effect of drugs and protect normal cells. Abnormalities in the course of the cell cycle and apoptosis, leading to uncontrolled cell proliferation and inhibition of differentiation, often occur in cancer cells⁵. Therefore, therapeutic strategies used in cancer treatment are often based on the induction of apoptosis and differentiation. Bioflavonoids, such as kaempferol, myricetin, luteolin or genistein, have a similar chemical structure to etoposide. Pre-treatment of mouse embryonic stem cell lines with topoisomerase II (Top II) catalytic inhibitor dexrazoxane and subsequent incubation

with kaempferol indicates that its anticancer activity is mostly Top II-independent⁶. These results indicate the need for a more detailed investigation of the direct effects of both etoposide and kaempferol on cancer cells.

We previously observed that kaempferol increased DNA damage induced by etoposide in acute promyelocytic leukemia HL-60 cell line⁷. Our earlier findings have led to the present investigation examining the effect of kaempferol and its glycoside derivatives on the apoptosis induced by etoposide in HL-60 cells, cell cycle progression, the production of reactive oxygen species (ROS), and the expression of *Nrf2* and *HO-1* genes. Furthermore, we tested the effect of kaempferol glycosides isolated from aerial parts of *Lens culinaris* Medik. (Fig. 1), which had not been examined before, on DNA damage induced by etoposide in HL-60 cells.

Materials and methods

Reagents

3,4',5,7-tetrahydroxyflavone (kaempferol) (K0133), 4'-demethylepipodophyllotoxin 9-(4,6-O-ethylidene- β -D-glucopyranoside) (etoposide) (E1383), low-melting-point (LMP) and normal-melting-point (NMP) agarose, DAPI (4',6-diamidino-2-phenylindole), dimethyl sulfoxide (DMSO), camptothecin (C9911), nocodazole (M1404), H₂DCFDA (2',7'-dichlorofluorescein diacetate), resazurin sodium salt (R7017) and hydrogen peroxide (H₂O₂) were purchased from Sigma-Aldrich (St. Louis, MO, USA). Kaempferol was dissolved in DMSO and stored at -20°C. Etoposide was dissolved in methanol. RNase A (DNase free) was purchased from EurX (Gdansk, Poland).

Kaempferol glycosides from the aerial parts of lentil

Kaempferol glycosides: kaempferol 3-O-[(6-O-E-caffeoyl)- β -D-glucopyranosyl-(1 \rightarrow 2)]- β -D-galactopyranoside-7-O- β -D-glucopyranoside (P2), kaempferol 3-O-[(6-O-E-p-coumaroyl)- β -D-glucopyranosyl-(1 \rightarrow 2)]- β -D-galactopyranoside-7-O- β -D-glucopyranoside (P5) and kaempferol 3-O-[(6-O-E-feruloyl)- β -D-glucopyranosyl-(1 \rightarrow 2)]- β -D-galactopyranoside-7-O- β -D-glucopyranoside (P7) were isolated from aerial parts of *Lens culinaris* Medik. according to the procedure described by Żuchowski et al. (2014)⁸. All isolated kaempferol glycosides were dissolved in 50% DMSO and stored at -20°C.

Cell preparation

The HL-60 (human promyelocytic leukemia) cell line was obtained from the American Type Culture Collection (ATCC). The cells were cultured in flasks at 37°C in 5% CO₂ atmosphere in Iscove's Modified Dulbecco's Medium (IMDM) with 2 mM L-glutamine, 25 mM HEPES (Lonza, Basel, Switzerland), 15% inactivated fetal bovine serum (FBS) and penicillin/streptomycin solution (100 U/ml and 100 μ g/ml, respectively).

Cell treatment

In all experiments the HL-60 cells were seeded in the culture medium and then incubated at 37°C with different concentrations (10-50 μ g/ml) of kaempferol and kaempferol derivatives: (P2), (P5) and (P7). The cells were also treated with different concentrations of etoposide (1 or 5 μ M) and incubated for 2 h at 37°C until DNA damage induction or for 24 h at 37°C to measure viability, apoptosis, cell cycle, ROS induction and gene expression. The final concentration of DMSO and methanol in the samples did not exceed 0.5%⁷.

Cell viability

Cell viability was measured using the resazurin reduction assay based on the ability of viable cells to reduce resazurin to fluorescent resorufin. The HL-60 cells were seeded on 96-well plates at density of 1×10^4 cells/ml in a culture medium and incubated for 24 h with the tested compounds (etoposide, kaempferol, P2, P5, P7) at 37°C in 5% CO₂. The assay was described in detail by Juszczak et al. (2020)⁹.

DNA damage

DNA damage was estimated using the alkaline comet assay according to the procedure defined by Singh et al. (1988)¹⁰, which was described in detail in the authors' previous work⁷.

Apoptosis

Apoptosis was measured using the FITC Annexin V Apoptosis Detection Kit II (BD Biosciences, San Jose, USA). The HL-60 cells were seeded in 6-well plates at density of 2×10^5 cells/ml. The cells incubated with 20 μM camptothecin (CAM) for 24 h at 37°C were the positive control. After incubation, the cells were collected and washed twice with ice-cold PBS. The cells were resuspended in 1 × Binding Buffer (100 μl) and incubated with FITC Annexin V (5 μl) and propidium iodide (PI) (5 μl) for 15 min at room temperature in the dark. Then, 400 μl of Binding Buffer was added to each tube and the samples were measured within 1 h using the LSRII flow cytometer (Becton Dickinson, San Jose, CA, USA) equipped with 488 nm laser excitation and BD FACSDiva software v 4.1.2. The percentage of apoptotic cells was expressed as a population of FITC Annexin V-positive cells¹¹.

Cell cycle

The HL-60 cells were seeded in 6-well plates at density of 0.5×10^6 cells/ml and incubated with the tested compounds. The cells incubated with 100 ng/ml nocodazol (NOC) for 24 h at 37°C were the positive control. Next, the cells were collected and washed twice with PBS. Then, the cells were resuspended in PBS and allowed to cool for 15 min on ice. Then, one volume of -20°C absolute ethanol was added and the samples were stored at 4°C. Before analysis samples were pelleted and resuspended in 300 μl of staining solution containing 40 μg/ml PI and 200 μg/ml RNase A. Samples were incubated for 30 min at 37°C in the dark until analysis. DNA content was analyzed using the LSRII flow cytometer (Becton Dickinson, San Jose, CA, USA)¹¹.

Detection of reactive oxygen species

The production of intracellular reactive oxygen species (ROS) was determined by measuring the fluorescence of 2',7'-dichlorofluorescein diacetate (H₂DCFDA). The cells (final density of 5×10^5 cells/ml) were seeded in 6-well plates and incubated with 5 μM etoposide and 10 μg/ml or 50 μg/ml kaempferol, P2, P5 and P7 derivative for 24 h at 37°C. The cells incubated for 15 min with 5 mM H₂O₂ at 37°C were the positive control. The assay was described in detail by Juszczak et al. (2020)⁹.

Gene expression analysis

To analyze the expression of *HO-1* and *Nrf2* genes the cells were seeded in 6-well plates and incubated with 1 μM or 5 μM etoposide and 10 μg/ml or 50 μg/ml kaempferol, P2, P5 and P7 derivative at 37°C for 24 h. Afterwards, the cells were collected and total RNA from each sample was extracted using the Universal RNA Purification Kit

(EurX, Gdansk, Poland), according to the manufacturer's instructions. The assay was described in detail by Juszcak et al. (2020)⁹.

Statistical analysis

The values of the comet assay were expressed as mean + standard error of the mean (SEM) from two experiments; data from the experiments were pooled and statistical parameters were calculated. The data from cell viability, apoptosis detection, cell cycle distribution and ROS measurement were presented as mean values \pm SD from 3-6 independent experiments. Statistical analyses were performed using GraphPad Prism 5 (GraphPad Software Inc., La Jolla, CA, USA). Statistical differences were determined by means of a one-way ANOVA analysis followed by *post hoc* Tukey's multiple comparison test. The differences were considered to be statistically significant when the *p* value was less than 0.05.

Expression of *HO-1* and *Nrf2* genes was calculated based on the double delta Ct method. Statistics were performed using a one-way ANOVA analysis followed by *post hoc* Dunnett multiple comparison test. The data were presented as a mean \pm SD, relative to control. *HO-1* and *Nrf2* expression was normalized to *GAPDH* gene expression.

Results and discussion

Different polyphenols, including kaempferol, have anticancer properties and can be used in cancer prevention and, probably, treatment. Flavonoids are found in plant material mainly in the form of glycosides¹². Therefore, we decided to investigate the effects of not only kaempferol but also its glycoside derivatives, which were isolated from aerial parts of *Lens culinaris* Medik., on the anticancer activity of etoposide in HL-60 cells. This is the first study that focuses on the effect of kaempferol and its glycosides on etoposide activity such as cytotoxicity, induction of apoptosis and DNA damage, cell cycle arrest, production of free radicals and expression of genes involved in the defense against oxidative stress.

Firstly, we observed that etoposide decreased the viability of HL-60 cells after 24 h incubation at all three tested concentrations (1 μ M, 5 μ M and 10 μ M) (Fig. 2A). We also observed that co-incubation of HL-60 cells with kaempferol and etoposide increased the cytotoxic effect of the drug notably. The incubation with 1 μ M etoposide and 50 μ g/ml kaempferol was more cytotoxic (69% of cell viability) than the incubation with only etoposide (83.2%) ($p < 0.001$) (Fig. 2A). Moreover, kaempferol with 5 μ M etoposide decreased cell viability from 58.2% to 50.6% and to 34% at 10 μ g/ml and 50 μ g/ml concentrations, respectively ($p < 0.001$). In the case of 10 μ M etoposide co-incubation with kaempferol at 10 μ g/ml and 50 μ g/ml concentrations decreased cell viability from 51.2% to 43.8% and to 30.8%, respectively ($p < 0.001$). Next, we investigated the impact of kaempferol and its glycosides (P2, P5, P7), isolated from aerial parts of *Lens culinaris* Medik., on the cytotoxic effects of etoposide (Fig. 2B-D). Kaempferol glycosides did not affect the cytotoxicity induced by etoposide in HL-60 cells. Only the P2 derivative decreased cell viability after incubation with 1 μ M etoposide from 85.2% to 79.8% ($p < 0.05$) and 71.6% ($p < 0.001$) at 10 μ g/ml and 50 μ g/ml concentrations, respectively (Fig. 2B). Studies carried out on the colon cancer LS174 cell line compared the cytotoxic activity of kaempferol and its analogs, i.e. kaempferol 3-O-glucoside and kaempferol 3-O-rutinoside isolated from the Tunisian quince *Cydonia oblonga* Miller¹³. Kaempferol, at the concentration of 120 μ M, induced more than 80% of growth inhibition after 72 h incubation, while this effect did not exceed 30% and 37% for kaempferol 3-O-glucoside and kaempferol 3-O-rutinoside,

respectively. Based on *in silico* analysis, it was suggested that these differences in antitumor activity between kaempferol and its analogs were caused by the absence of glucosyl groups in a kaempferol molecule.

Additionally, we examined the effect of etoposide, kaempferol and its glycoside derivatives on the morphology of HL-60 cells using phase-contrast microscopy (Fig. 3A-C). Firstly, we observed that 5 μM etoposide decreased the number of HL-60 cells and the cells became rough with shrinkage in comparison to the control cells. Moreover, the cells incubated with etoposide did not form clusters (Fig. 3A). Cells become enlarged and some of them have a fragmented nucleus. Similar changes in cell morphology were caused after incubation with 20 μM camptothecin (CAM). Kaempferol also changed the morphology of cells, making them rough and not clustering like control cells. Co-incubation with etoposide and kaempferol led to a reduction in the number of cells and did not change their morphology. These results are consistent with our examination of HL-60 cells viability (Fig. 2). We observed that kaempferol derivatives did not change the morphology of HL-60 cells (Fig. 3B). Moreover, we detected that kaempferol derivatives protected HL-60 cells against morphological changes induced by etoposide (Fig. 3C).

Next, we tested the level of DNA damage following exposure to kaempferol derivatives and etoposide. Kaempferol alone induced DNA damage in HL-60 cells as well as increased DNA damage induced by etoposide⁷. Previously, we showed that co-incubation of HL-60 cells with 1 μM etoposide and 50 $\mu\text{g/ml}$ kaempferol increased the level of DNA damage from 27.5% to 39.6%. In these studies, we did not observe any changes in the level of DNA damage induced by etoposide in HL-60 cells incubated with the two tested kaempferol derivatives (P2 and P5) (Fig. 4). Fig. 5 shows representative photos of the comets obtained after the incubation of HL-60 cells with these kaempferol derivatives (10-50 $\mu\text{g/ml}$) and 1 μM etoposide. The presented data are consistent with our previous results for two other kaempferol derivatives isolated from *Lens culinaris* Medik.⁷.

To investigate whether a drop in the viability of HL-60 cells, which we observed during the co-incubation with kaempferol and etoposide, was due to an increase in programmed cell death, we examined the level of apoptotic HL-60 cells after incubation (24 h) with 5 μM etoposide, 10-50 $\mu\text{g/ml}$ kaempferol, kaempferol derivatives (P2, P5, P7) and with combinations of those compounds. The cells incubated with 20 μM camptothecin (CAM) were the positive control. Our results indicate that kaempferol does not have an impact on the level of apoptosis induced by etoposide in HL-60 cells (Fig. 6A). Hence, an increase in the cytotoxic effect of etoposide after co-incubation with kaempferol is not associated with apoptosis. Studies carried out on HL-60 cells confirmed that quercetin protects cells from apoptosis induced by etoposide¹⁴. On the other hand, another polyphenol curcumin significantly enhances apoptosis induced by etoposide in HL-60 cells¹⁵.

We observed that all three tested kaempferol glycosides did not induce apoptosis in HL-60 cells by itself (Fig. 6B-D). The opposite effect on apoptosis of U937, K562, and HL-60 cells was observed in the case of the kaempferol glycoside isolated from *Wattakaka volubilis*¹⁶. Moreover, we noticed that P2 derivative at the concentration of 50 $\mu\text{g/ml}$ reduced the level of apoptosis induced by etoposide from 35.8% to 26.3% ($p < 0.001$) (Fig. 6B). Similarly, P7 derivative decreased the level of apoptotic cells induced by etoposide from 35.8% to 29.8% ($p < 0.05$) (Fig. 6D).

Under our conditions, we observed that kaempferol did not induce apoptosis in HL-60 cells (Fig. 6A). Moradzadeh et al. showed that kaempferol at the concentrations of 50 and 100 μM decreased the viability of HL-60 cells after 72 h incubation¹⁷. Additionally, incubation with kaempferol for 72 h enhanced apoptosis in HL-60 cells via both intrinsic and extrinsic pathways. In our study we did not observe any pro-apoptotic effect of

kaempferol, probably due to a much shorter incubation time (24 h). It was shown that kaempferol decreased the viability and induced the apoptosis of HepG2 hepatocellular carcinoma cells¹⁸. Kaempferol also reduced the viability and increased the level of apoptosis in human cervical cancer (HeLa) cells¹⁹. These studies also showed that kaempferol had no toxic effect on normal human foreskin fibroblast (HFF) cells. Kaempferol derived from *Semecarpus anacardium* protected normal lung and liver cells from apoptosis induced by H₂O₂²⁰. This protective effect was associated with an increased expression of proteins responsible for the response to oxidative stress, like Nrf2, superoxide dismutase (SOD), catalase and phospho-p38 MAPK.

Next, we investigated the cell cycle progression in HL-60 cells after 24 h incubation with etoposide, kaempferol and its glycoside derivatives (Fig. 7). We observed that both kaempferol and its glycoside derivatives did not alter the progression of cell cycle. We also observed increase of cell level in sub-G1 phase from 1.1% to 10.5% after incubation with 0.5 μ M etoposide ($p < 0.01$). Moreover, the G0/G1 fraction decreased significantly in response to 0.5 μ M etoposide compared to control cells from 42.4% to 20% ($p < 0.001$). The presence of cells in the sub-G1 phase is associated with apoptosis and DNA fragmentation. This result confirms the strong apoptotic effect of etoposide, as shown also in the experiment with double staining of cells with annexin V and propidium iodide (Fig. 6). Our results are in agreement with data obtained by Żuryń and colleagues on HL-60 cells treated with 0.5-1 μ M etoposide²¹. We also observed a slight decrease in the number of S phase cells after incubation with etoposide ($p < 0.05$)²⁰. Additionally, etoposide increased the population of cells in G2/M phase from 24.4% to 50.2% ($p < 0.001$). We noticed that both kaempferol and its glycoside derivatives had no impact on progression of cell cycle in cells incubated with etoposide (Fig. 7).

Kaempferol increases the antioxidant defense against free radicals and leads to the reduction of cancer risk¹. We decided to examine the production of intracellular ROS after 24 h incubation of HL-60 cells with etoposide, kaempferol and its derivatives. We used the H₂DCF-DA probe to determine the effect of these compounds on the intracellular redox status. Firstly, we observed that 5 μ M etoposide induced the statistically significant increase of the level of intracellular ROS ($p < 0.001$) (Fig. 8). It confirms that etoposide at this concentration induces oxidative stress in HL-60 cells. Next, we investigated the induction of intracellular ROS in the cells treated with 10-50 μ g/ml kaempferol or its glycoside derivatives (P2, P5, P7) and in combination with 5 μ M etoposide. We observed that 50 μ g/ml kaempferol decreased the level of intracellular ROS in HL-60 cells ($p < 0.001$) compared to the control cells, which indicates that kaempferol reduces endogenous free radicals (Fig. 8A). Moreover, 50 μ g/ml kaempferol decreased the level of ROS induced by 5 μ M etoposide ($p < 0.001$) (Fig. 8A). We did not observe any changes in ROS induction by etoposide in the case of 10 μ g/ml kaempferol. The presented results showed that the enhancement of etoposide cytotoxicity by kaempferol was not due an increase in ROS generation. The antioxidant activity of kaempferol does not limit the activity of the drug. It was shown that kaempferol isolated from *Semecarpus anacardium* stem bark, reduces the number of free radicals induced by H₂O₂ in the normal cells of the lungs and liver²⁰. The antioxidant activity of kaempferol was also remarked in a study conducted on LS174 colon cancer cells, which showed that kaempferol at 75 μ M reduced ROS production¹³. The incubation of parental and 5-fluorouracil-resistant LS174 cells with 75 μ M kaempferol reduced ROS production by 69% and 56%, respectively. Moreover, co-incubation with kaempferol and 5-fluorouracil offering anti-cancer properties enhanced the inhibitory effect on ROS production in both types of cells¹³. Riahi-Chebbi et al. (2019) showed that kaempferol decreased the viability of cancer LS174 cells and enhanced the cytotoxic effect of 5-fluorouracil after 72 h incubation¹³.

Interestingly, we observed that the P2 derivative increased the level of intracellular ROS at the concentration of 10 $\mu\text{g/ml}$ compared to the control cells ($p < 0.01$) (Fig. 8B). Moreover, co-incubation of 5 μM etoposide with 10 $\mu\text{g/ml}$ P2 and P5 at 10 and 50 $\mu\text{g/ml}$ elevated the ROS level in comparison to the incubation only with etoposide ($p < 0.001$) (Fig. 8B and C). However, this increase in ROS generation did not increase the cytotoxicity of etoposide. On the other hand, P5 at the concentration of 50 $\mu\text{g/ml}$ decreased the ROS level to 77% compared to the control ($p < 0.01$) (Fig. 8C). In contrast to P2 and P5, P7 derivative significantly decreased the level of ROS induced by etoposide ($p < 0.01$) (Fig. 8D). Fig. 9 shows photos of cells loaded with the $\text{H}_2\text{DCF-DA}$ probe.

The nuclear factor erythroid 2-related factor 2 (Nrf2) is a key cytoprotective molecule responsible for regulating the expression of antioxidant proteins, including heme oxygenase-1 (HO-1)²². On the one hand, *Nrf2* silencing increases the sensitivity of cancer cells to drugs and *Nrf2* activation triggers antioxidant pathways that protect cancer cells^{23,24}. HO-1 catalyzes heme degradation to biliverdin, carbon oxide (CO) and iron ions. Although the main mechanism of HO-1 activity is related to heme metabolism, HO-1 also plays a role in the cellular response to oxidative stress²¹.

We noticed that etoposide increased the expression of *HO-1* gene 4.9-fold and 6.5-fold ($p < 0.001$) at 1 μM and 5 μM concentrations, respectively (Fig. 10). Moreover, kaempferol induced a 1.4-fold and 2.5-fold increase of *HO-1* gene expression at 10 $\mu\text{g/ml}$ and 50 $\mu\text{g/ml}$ concentrations ($p < 0.05$ and $p < 0.001$, respectively) (Fig. 11A). We did not observe any changes in *HO-1* gene expression after incubation with all kaempferol glycoside derivatives except a minor increase at 50 $\mu\text{g/ml}$ P2 ($p < 0.05$) (Fig. 11B). Next, we tested the expression of the *Nrf2* gene under the same incubation conditions. We did not notice any impact of etoposide (Fig. 10) and kaempferol on the level of *Nrf2* gene expression (Fig. 11A). Only in the case of 50 $\mu\text{g/ml}$ P5 and 10 $\mu\text{g/ml}$ P7 derivatives we observed a minor decrease in *Nrf2* mRNA expression (Fig. 11C and D). It was shown that flavonoids isolated from *Petasites japonicus*, which included, among others, kaempferol-3-O-(6''-acetyl)- β -D-glucoside and kaempferol-3-O- β -D-glucoside, activated the *Nrf-2* and *HO-1* genes²⁵. An extract from graviola leaves – rich in kaempferol-rutinoside – increased the expression of *Nrf2* in HepG2 liver cancer cells but did not affect the expression of the *HO-1* gene²⁶.

Conclusions

Our results indicate that kaempferol increases the sensitivity of HL-60 cells to etoposide but does not increase of apoptosis induced by etoposide. Moreover, kaempferol decreases ROS generation by etoposide, which may be related to the induction of *HO-1* gene expression. Our study also shows that glycoside kaempferol derivatives, isolated from *Lens culinaris* Medik., can limit the apoptotic activity of etoposide in cancer HL-60 cells. Glycoside derivatives of kaempferol may have an opposite effect on the action of etoposide in HL-60 cells compared to kaempferol. Our results indicate the need for further and more detailed research into the interactions between polyphenols and chemotherapeutic agents used in the treatment of cancer.

Acknowledgments This work was supported financially by the University of Lodz, Poland, the Faculty of Biology and Environmental Protection.

Compliance with ethical standards

Conflict of interest The authors declare no conflict of interest.

References

1. Chen, A.Y., Chen, Y.C. A review of the dietary flavonoid, kaempferol on human health and cancer chemoprevention. *Food Chem* 138:2099-2107, <https://doi:10.1016/j.foodchem.2012.11.139> (2013).
2. Zhou, Y., Zheng, J., Li, Y., Xu, D.P., Li, S., Chen, Y.M., Li, H.B. Natural Polyphenols for Prevention and Treatment of Cancer. *Nutrients* 8ii:E515, <https://doi:10.3390/nu8080515> (2016).
3. Imran, M., Salehi, B., Sharifi-Rad, J., Aslam Gondal, T., Saeed, F., Imran, A., Shahbaz, M., Tsouh Fokou, P.V., Umair Arsha, M., Khan, H., Guerreiro, S.G., Martins, N., Estevinho, L.M. Kaempferol: A Key Emphasis to Its Anticancer Potential. *Molecules* 24:2277, <https://doi:10.3390/molecules24122277> (2019).
4. Montecucco, A., Zanetta, F., Biamonti, G. Molecular mechanisms of etoposide. *EXCLI J* 14:95-108, <https://doi:10.17179/excli2015-561> (2015).
5. He, M., Zhou, W., Li, C., Guo, M. MicroRNAs, DNA Damage Response, and Cancer Treatment. *Int J Mol Sci* 17:pii:E2087, <https://doi:10.3390/ijms17122087> (2016).
6. Goodenow, D., Emmanuel, F., Berman, C., Sahyouni, M., Richardson, C. Bioflavonoids cause DNA double-strand breaks and chromosomal translocations through topoisomerase II-dependent and -independent mechanisms. *Mutat Res* 849:503144, <https://doi:10.1016/j.mrgentox.2020.503144> (2020).
7. Kluska, M., Juszczak, M., Wysokiński, D., Żuchowski, J., Stochmal, A., Woźniak, K. Kaempferol derivatives isolated from *Lens culinaris* Medik. reduce DNA damage induced by etoposide in peripheral blood mononuclear cells. *Toxicol Res* 8:896-907, <https://doi:10.1039/c9tx00176j> (2019).
8. Żuchowski, J., Pecio, Ł., Stochmal, A. Novel flavonol glycosides from the aerial parts of lentil (*Lens culinaris*). *Molecules* 19:18152-18178, <https://doi:10.3390/molecules191118152> (2014).
9. Juszczak, M., Kluska, M., Wysokiński, D., Woźniak, K. DNA damage and antioxidant properties of CORM-2 in normal and cancer cells. *Sci Rep* 10:12200, <https://doi:10.1038/s41598-020-68948-6> (2020).
10. Singh, N.P., McCoy, T., Tice, R.R., Schneider, E.L. A simple technique for quantitation of low levels of DNA damage in individual cells. *Exp Cell Res* 175:184-192, [https://doi:10.1016/0014-4827\(88\)90265-0](https://doi:10.1016/0014-4827(88)90265-0) (1988).
11. Macieja, A., Kopa, P., Galia, G., Pastwa, E., Majsterek, I., Popławski, T. Comparison of the effect of three different topoisomerase II inhibitors combined with cisplatin in human glioblastoma cells sensitized with double strand break repair inhibitors. *Mol Biol Rep* 46:3625-3636, <https://doi:10.1007/s11033-019-04605-0> (2019).
12. Sak, K. Cytotoxicity of dietary flavonoids on different human cancer types. *Pharmacognosy Rev* 8:122-146, <https://doi:10.4103/0973-7847.134247> (2014).
13. Riahi-Chebbi, I., Souid, S., Othman, H., Haoues, M., Karoui, H., Morel, A., Srairi-Abid, N., Essafi, M., Essafi-Benkhadir, K. The Phenolic compound Kaempferol overcomes 5-fluorouracil resistance in human resistant LS174 colon cancer cells. *Sci Rep* 9:195, <https://doi:10.1038/s41598-018-36808-z> (2019).
14. Papież, M., Krzyściak, W. The antioxidant quercetin protects HL-60 cells with high myeloperoxidase activity against pro-oxidative and apoptotic effects of etoposide. *Acta Biochem Pol* 61:795-799, (2014).
15. Papież, M.A., Krzyściak, W., Szade, K., Bukowska-Straková, K., Kozakowska, M., Hajduk, K., Bystrowska, B., Dulak, J., Jozkowicz, A. Curcumin enhances the cytogenotoxic effect of etoposide in leukemia cells through

- induction of reactive oxygen species. *Drug Des Devel Ther* 10:557-570, <https://doi:10.2147/DDDT.S92687> (2016).
16. Nandi, D., Besra, S.E., Vedasiromoni, J.R., Giri, V.S., Rana, P., Jaisankar, P. Anti-leukemic activity of *Wattakaka volubilis* leaf extract against human myeloid leukemia cell lines. *J Ethnopharmacol* 144:466-473, <https://doi:10.1016/j.jep.2012.08.021> (2012).
 17. Moradzadeh, M., Tabarraei, A., Sadeghnia, H.R., Ghorbani, A., Mohamadkhani, A., Erfanian, S., Sahebkar, A. Kaempferol increases apoptosis in human acute promyelocytic leukemia cells and inhibits multidrug resistance genes. *J Cell Biochem* 119:2288-2297, <https://doi:10.1002/jcb.26391> (2018).
 18. Guo, H., Ren, F., Zhang, L., Zhang, X., Yang, R., Xie, B., Li, Z., Hu, Z., Duan, Z., Zhang, J. Kaempferol induces apoptosis in HepG2 cells via activation of the endoplasmic reticulum stress pathway. *Mol Med Rep* 13:2791-2800, <https://doi:10.3892/mmr.2016.4845> (2016).
 19. Kashafi, E., Moradzadeh, M., Mohamadkhani, A., Erfanian, S. Kaempferol increases apoptosis in human cervical cancer HeLa cells via PI3K/AKT and telomerase pathways. *Biomed Pharmacother* 89:573-577, <https://doi:10.1016/j.biopha.2017.02.061> (2017).
 20. Kumar, A.D., Bevara, G.B., Kaja, L.K., Badana, A.K., Malla, R.R. Protective effect of 3-O-methyl quercetin and kaempferol from *Semecarpus anacardium* against H₂O₂ induced cytotoxicity in lung and liver cells. *BMC Complement Altern Med* 16:376, <https://doi:10.1186/s12906-016-1354-z> (2016).
 21. Żuryń, A., Krajewski, A., Szulc, D., Litwiniec, A., Grzanka, A. Activity of cyclin B1 in HL-60 cells treated with etoposide. *Acta Histochemica* 118:537-543, <https://doi:10.1016/j.acthis.2016.05.010> (2016).
 22. Loboda, A., Damulewicz, M., Pyza, E., Jozkowicz, A., Dulak, J. Role of Nrf2/HO-1 system in development, oxidative stress response and diseases: an evolutionarily conserved mechanism. *Cell Mol Life Sci* 73:3221-3247, <https://doi:10.1007/s00018-016-2223-0> (2016).
 23. Wang, X.J., Sun, Z., Villeneuve, N.F., Zhang, S., Zhao, F., Li, Y., Chen, W., Yi, X., Zheng, W., Wondrak, G.T., Wong, P.K., Zhang, D.D. Nrf2 enhances resistance of cancer cells to chemotherapeutic drugs, the dark side of Nrf2. *Carcinogenesis* 29:1235-1243, <https://doi:10.1093/carcin/bgn095> (2008).
 24. Ma, X., Zhang, J., Liu, S., Huang, Y., Chen, B., Wang, D. Nrf2 knockdown by shRNA inhibits tumor growth and increases efficacy of chemotherapy in cervical cancer. *Cancer Chemother Pharmacol* 69:485-494, <https://doi:10.1007/s00280-011-1722-9> (2012).
 25. Kim, K.M., Im, A.R., Lee, S., Chae, S. Dual Protective Effects of Flavonoids from *Petasites japonicus* against UVB-Induced Apoptosis Mediated via HSF-1 Activated Heat Shock Proteins and Nrf2-Activated Heme Oxygenase-1 Pathways. *Biol Pharm Bull* 40:765-773, <https://doi:10.1248/bpb.b16-00691> (2017).
 26. Son, Y.R., Choi, E.H., Kim, G.T., Park, T.S., Shim, S.M. Bioefficacy of Graviola leaf extracts in scavenging free radicals and upregulating antioxidant genes. *Food Funct* 7:861-871, <https://doi:10.1039/c5fo01258a> (2016).

The legends for the figures

Fig. 1. Chemical structures of kaempferol and its derivatives isolated from *Lens culinaris* Medik. (A) kaempferol; (B) kaempferol 3-O-[(6-O-E-caffeoyl)-β-D-glucopyranosyl-(1→2)]-β-D-galactopyranoside-7-O-β-D-glucopyranoside (P2); (C) kaempferol 3-O-[(6-O-E-p-coumaroyl)-β-D-glucopyranosyl-(1→2)]-β-D-

- galactopyranoside-7-O- β -D-glucopyranoside (P5); (D) kaempferol 3-O-[(6-O-E-feruloyl)- β -D-glucopyranosyl-(1 \rightarrow 2)]- β -D-galactopyranoside-7-O- β -D-glucopyranoside (P7).
- Fig. 2. Viability of HL-60 cells determined by resazurin reduction assay after 24 h treatment with 1-10 μ M etoposide (E) and 10-50 μ g/ml kaempferol (K) (A), P2 (B), P5 (C) and P7 (D) derivative. The figure shows mean results \pm SD, n = 6; * p < 0.05, ** p < 0.01, *** p < 0.001.
- Fig. 3. Morphological changes of HL-60 cells as examined by phase-contrast microscopy (magnification, 200 \times) after incubation with kaempferol and etoposide (A), kaempferol derivatives (B) or kaempferol derivatives and etoposide (C). Cells with fragmented nucleus (I), enlarged cells (II).
- Fig. 4. DNA damage, measured as the comet tail DNA (%) of HL-60 cells incubated for 2 h at 37 $^{\circ}$ C with P2 (A) and P5 (B) derivative (10-50 μ g/ml) and 1 μ M etoposide (E), analyzed by the alkaline comet assay. The figure shows mean results \pm SEM, n = 100; * p < 0.05, ** p < 0.01, *** p < 0.001.
- Fig. 5. Representative pictures of comets, obtained in the alkaline version of the comet assay after incubation of HL-60 cells with 10 μ g/ml or 50 μ g/ml P2 and P5 kaempferol derivatives and 1 μ M etoposide (E). The figure also contains pictures of comets from negative control (Ctrl) and positive control (cells incubated with H₂O₂ at 20 μ M for 15 min on ice).
- Fig. 6. Apoptosis measured by flow cytometry using a double staining of FITC Annexin V and propidium iodide in HL-60 cells incubated for 24 h at 37 $^{\circ}$ C with 5 μ M etoposide (E) and 10 μ g/ml or 50 μ g/ml kaempferol (K) (A), P2 (B), P5 (C) and P7 (D) derivative. The cells incubated with 20 μ M camptothecin (CAM) for 24 h at 37 $^{\circ}$ C were positive control. The figure shows mean results \pm SD, n = 3; * p < 0.05, ** p < 0.01, *** p < 0.001.
- Fig. 7. Cell cycle distribution measured by flow cytometry using a staining with propidium iodide in HL-60 cells incubated for 24 h at 37 $^{\circ}$ C with 0.5 μ M etoposide (E) and 10 μ g/ml or 50 μ g/ml kaempferol (K) (A), P2 (B), P5 (C) and P7 (D) derivative. The cells incubated with 100 ng/ml nocodazole (NOC) for 24 h at 37 $^{\circ}$ C were positive control. The figure shows mean results \pm SD, n = 3; * p < 0.05, ** p < 0.01, *** p < 0.001.
- Fig. 8. Reactive oxygen species (ROS) level in HL-60 cells incubated for 24 h at 37 $^{\circ}$ C with 5 μ M etoposide (E) and 10 μ g/ml or 50 μ g/ml kaempferol (K) (A), P2 (B), P5 (C) and P7 (D) derivative. The cells incubated with 5 mM H₂O₂ for 15 min at 37 $^{\circ}$ C were positive control. The figure shows mean results \pm SD, n = 6; * p < 0.05, ** p < 0.01, *** p < 0.001.
- Fig. 9. Representative photos of cells with 20 the fluorescence probe H₂DCFH-DA after 24 h incubation at 37 $^{\circ}$ C with 5 μ M etoposide (E) and 10 μ g/ml or 50 μ g/ml kaempferol (K). The figure also contains pictures of comets from negative control (Ctrl).
- Fig. 10. Relative expression of *HO-1* and *Nrf2* genes in HL-60 cells incubated for 24 h at 37 $^{\circ}$ C with 1 μ M or 5 μ M etoposide (E). The figure shows mean results \pm SD, n = 4; *** p < 0.001.
- Fig. 11. Relative expression of *HO-1* and *Nrf2* genes in HL-60 cells incubated for 24 h at 37 $^{\circ}$ C with 10 μ g/ml or 50 μ g/ml kaempferol (K) (A), P2 (B), P5 (C) and P7 (D) derivative. The figure shows mean results \pm SD, n = 4; * p < 0.05, ** p < 0.01, *** p < 0.001.

Figures

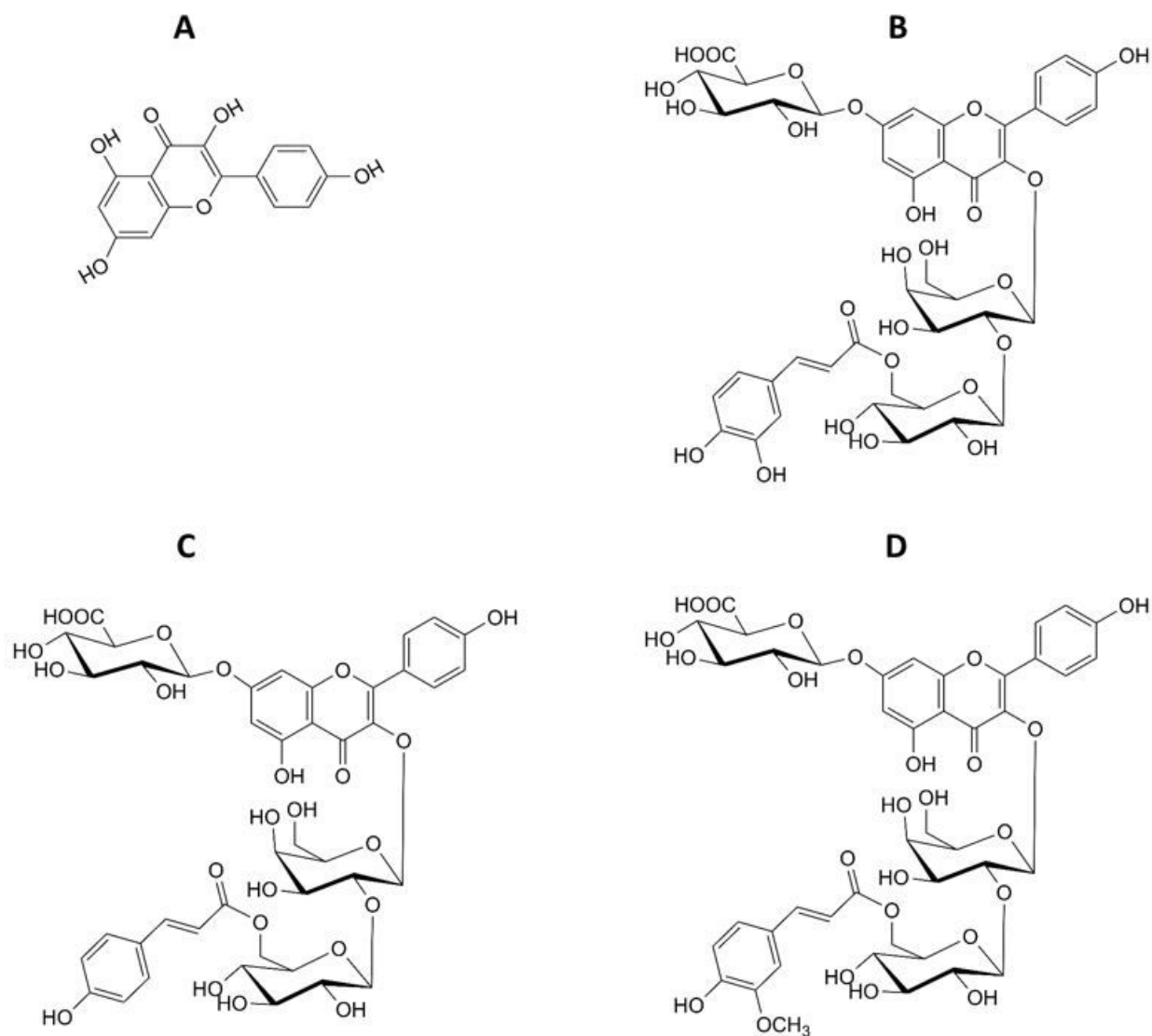


Figure 1

Chemical structures of kaempferol and its derivatives isolated from *Lens culinaris* Medik. (A) kaempferol; (B) kaempferol 3-O-[(6-O-E-caffeoyl)- β -D-glucopyranosyl-(1 \rightarrow 2)]- β -D-galactopyranoside-7-O- β -D-glucopyranoside (P2); (C) kaempferol 3-O-[(6-O-E-p-coumaroyl)- β -D-glucopyranosyl-(1 \rightarrow 2)]- β -D-galactopyranoside-7-O- β -D-glucopyranoside (P5); (D) kaempferol 3-O-[(6-O-E-feruloyl)- β -D-glucopyranosyl-(1 \rightarrow 2)]- β -D-galactopyranoside-7-O- β -D-glucopyranoside (P7).

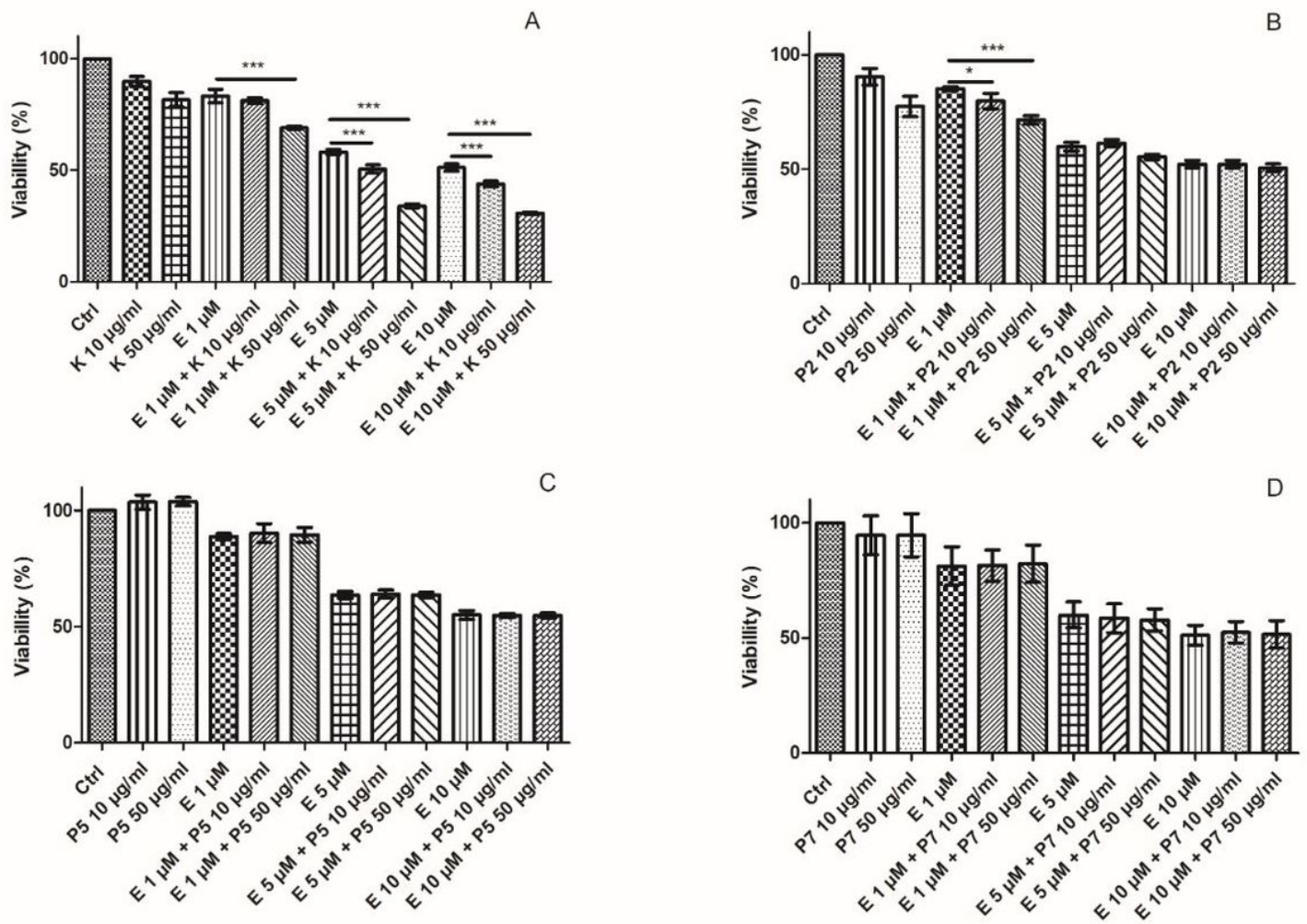


Figure 2

Viability of HL-60 cells determined by resazurin reduction assay after 24 h treatment with 1-10 μM etoposide (E) and 10-50 $\mu\text{g/ml}$ kaempferol (K) (A), P2 (B), P5 (C) and P7 (D) derivative. The figure shows mean results \pm SD, $n = 6$; * $p < 0.05$, ** $p < 0.01$, *** $p < 0.001$.

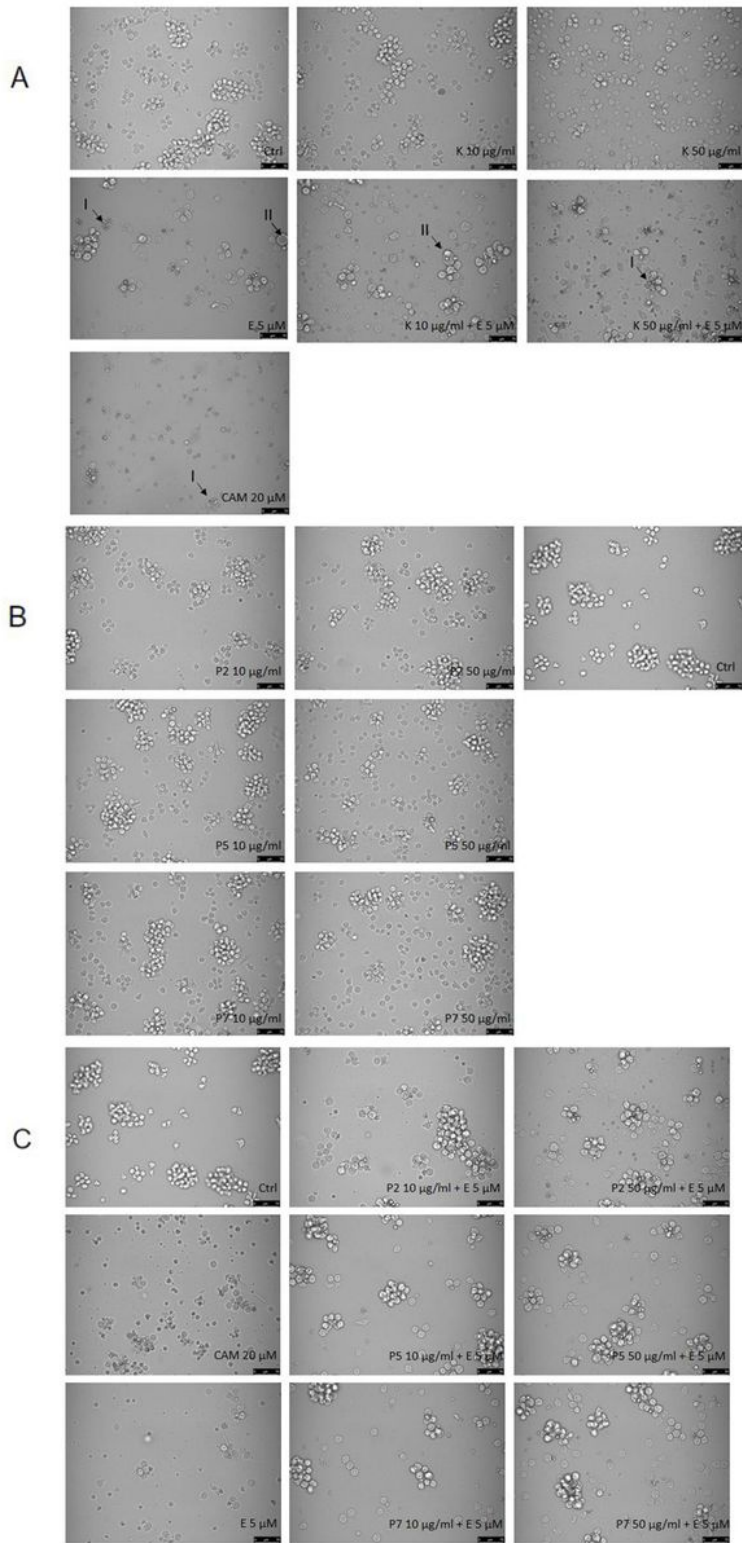


Figure 3

Morphological changes of HL-60 cells as examined by phase-contrast microscopy (magnification, 200 \times) after incubation with kaempferol and etoposide (A), kaempferol derivatives (B) or kaempferol derivatives and etoposide (C). Cells with fragmented nucleus (I), enlarged cells (II).

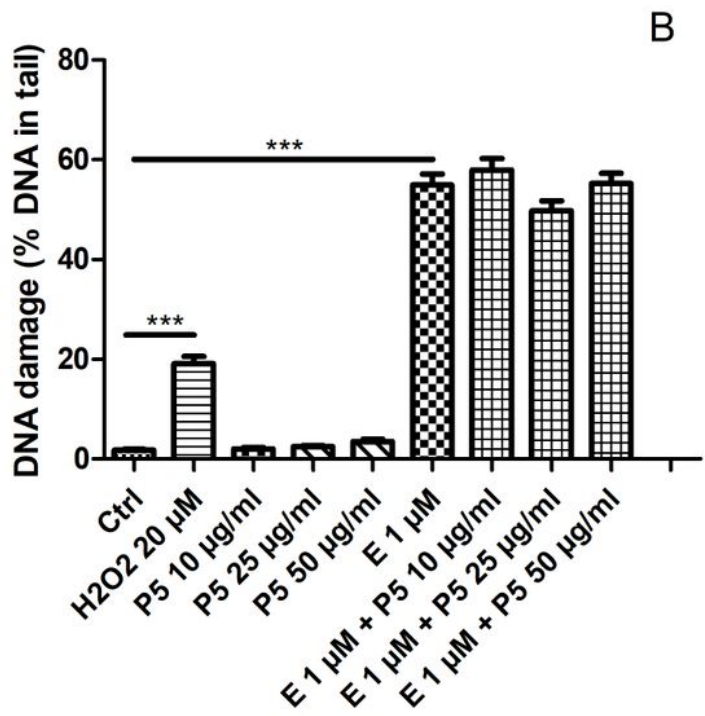
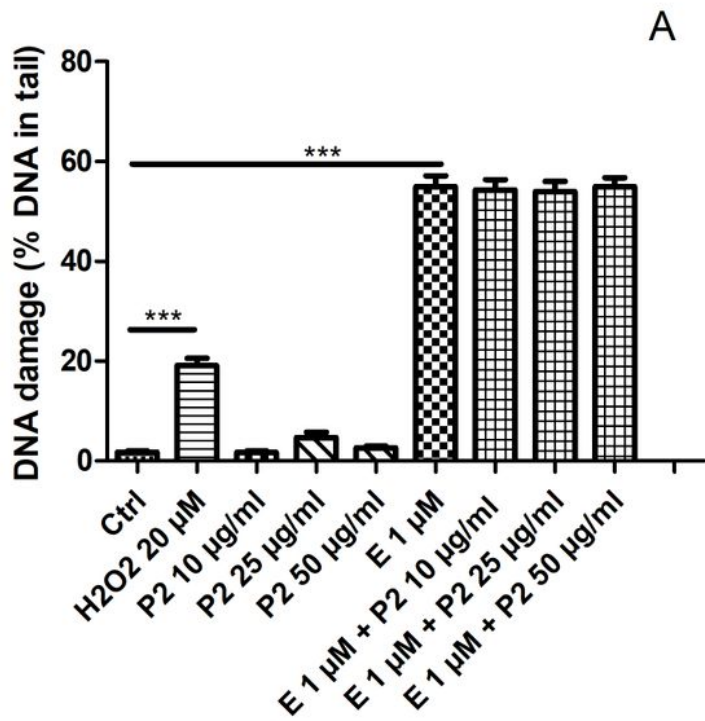


Figure 4

DNA damage, measured as the comet tail DNA (%) of HL-60 cells incubated for 2 h at 37°C with P2 (A) and P5 (B) derivative (10-50 µg/ml) and 1 µM etoposide (E), analyzed by the alkaline comet assay. The figure shows mean results \pm SEM, $n = 100$; * $p < 0.05$, ** $p < 0.01$, *** $p < 0.001$.

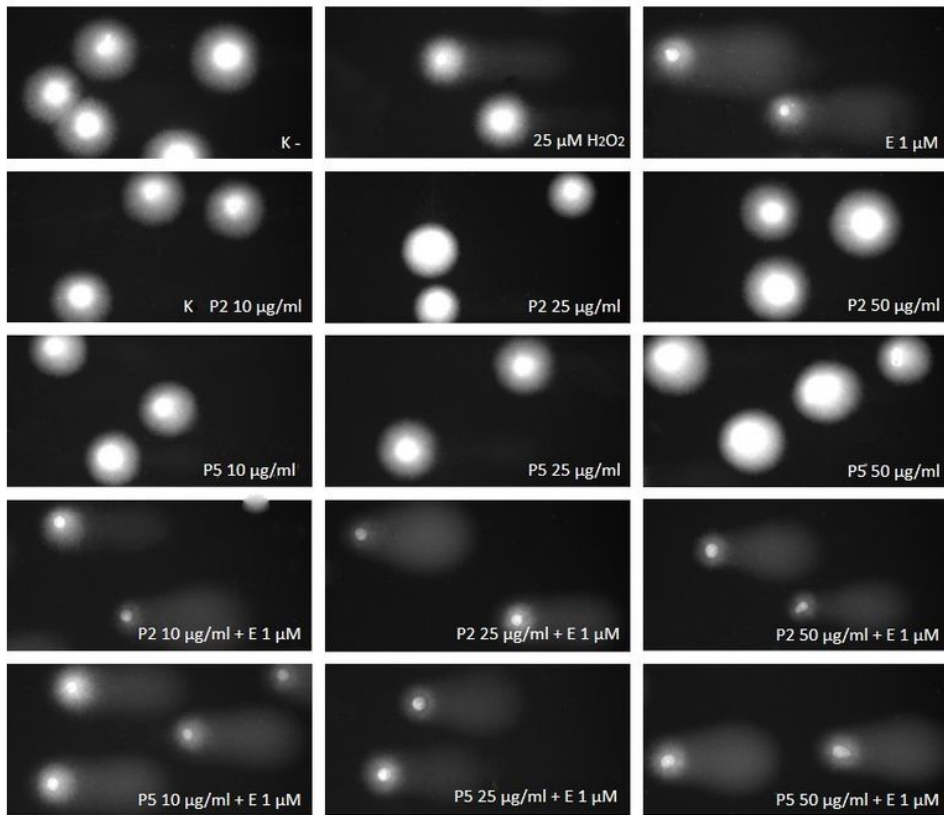


Figure 5

Representative pictures of comets, obtained in the alkaline version of the comet assay after incubation of HL-60 cells with 10 $\mu\text{g/ml}$ or 50 $\mu\text{g/ml}$ P2 and P5 kaempferol derivatives and 1 μM etoposide (E). The figure also contains pictures of comets from negative control (Ctrl) and positive control (cells incubated with H₂O₂ at 20 μM for 15 min on ice).

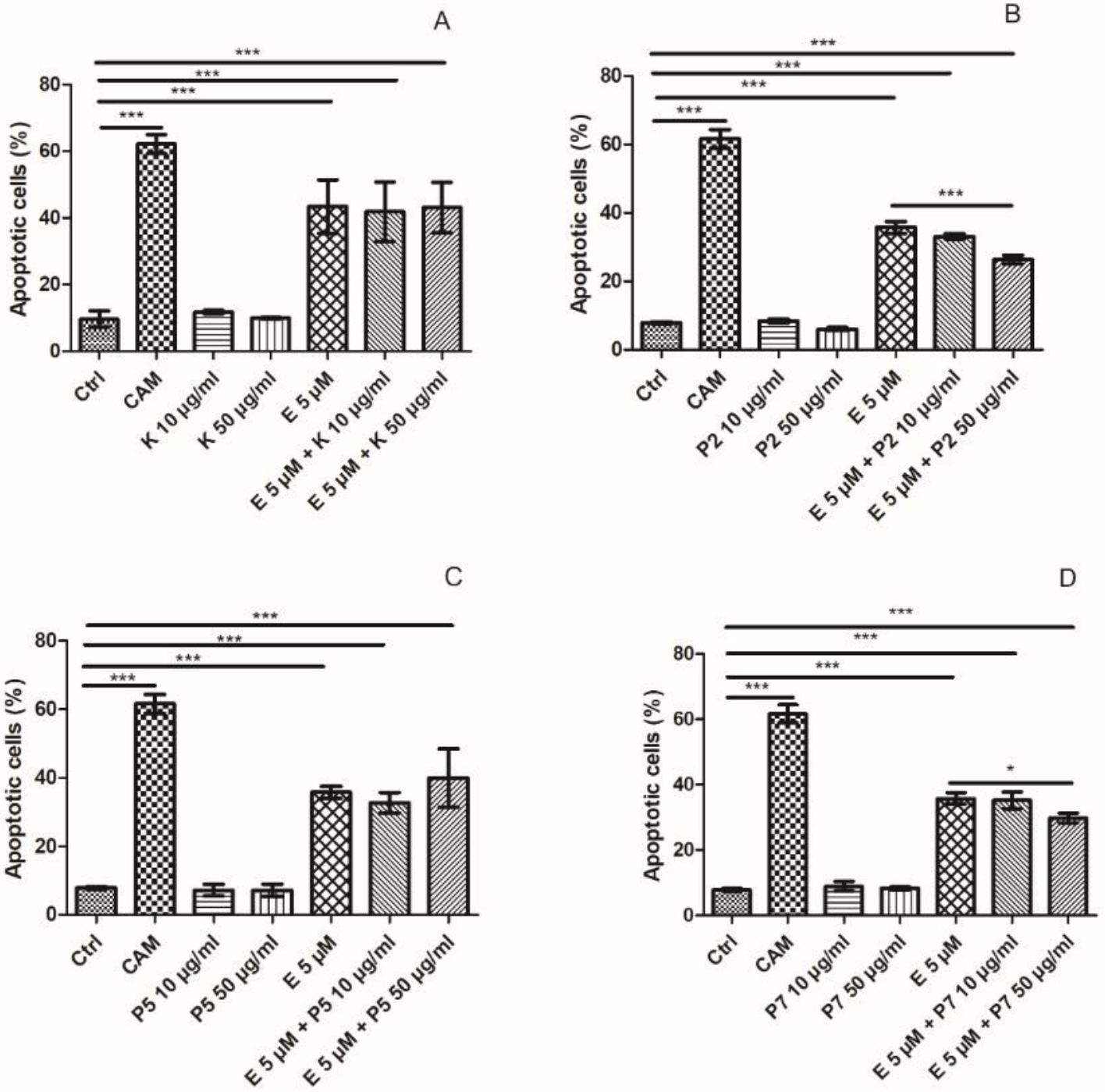


Figure 6

Apoptosis measured by flow cytometry using a double staining of FITC Annexin V and propidium iodide in HL-60 cells incubated for 24 h at 37°C with 5 µM etoposide (E) and 10 µg/ml or 50 µg/ml kaempferol (K) (A), P2 (B), P5 (C) and P7 (D) derivative. The cells incubated with 20 µM camptothecin (CAM) for 24 h at 37°C were positive control. The figure shows mean results ± SD, n = 3; * p < 0.05, ** p < 0.01, *** p < 0.001.

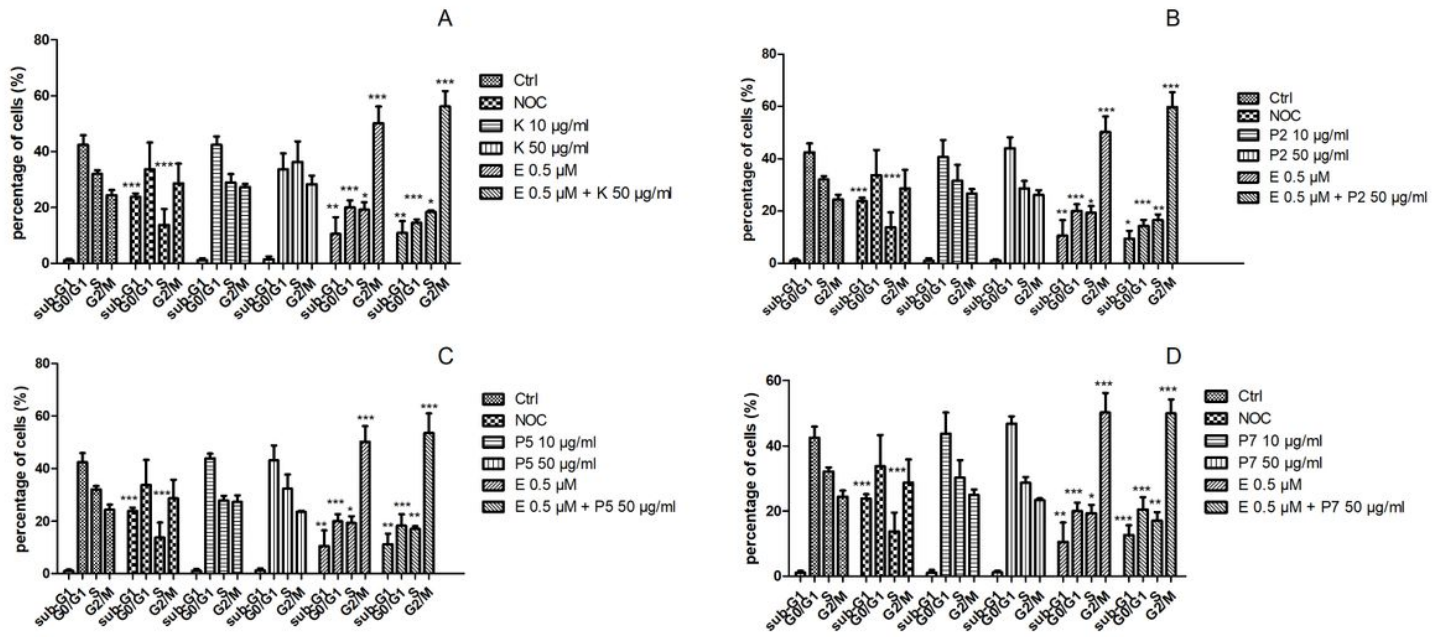


Figure 7

Cell cycle distribution measured by flow cytometry using a staining with propidium iodide in HL-60 cells incubated for 24 h at 37°C with 0.5 µM etoposide (E) and 10 µg/ml or 50 µg/ml kaempferol (K) (A), P2 (B), P5 (C) and P7 (D) derivative. The cells incubated with 100 ng/ml nocodazole (NOC) for 24 h at 37°C were positive control. The figure shows mean results \pm SD, n = 3; * p < 0.05, ** p < 0.01, *** p < 0.001.

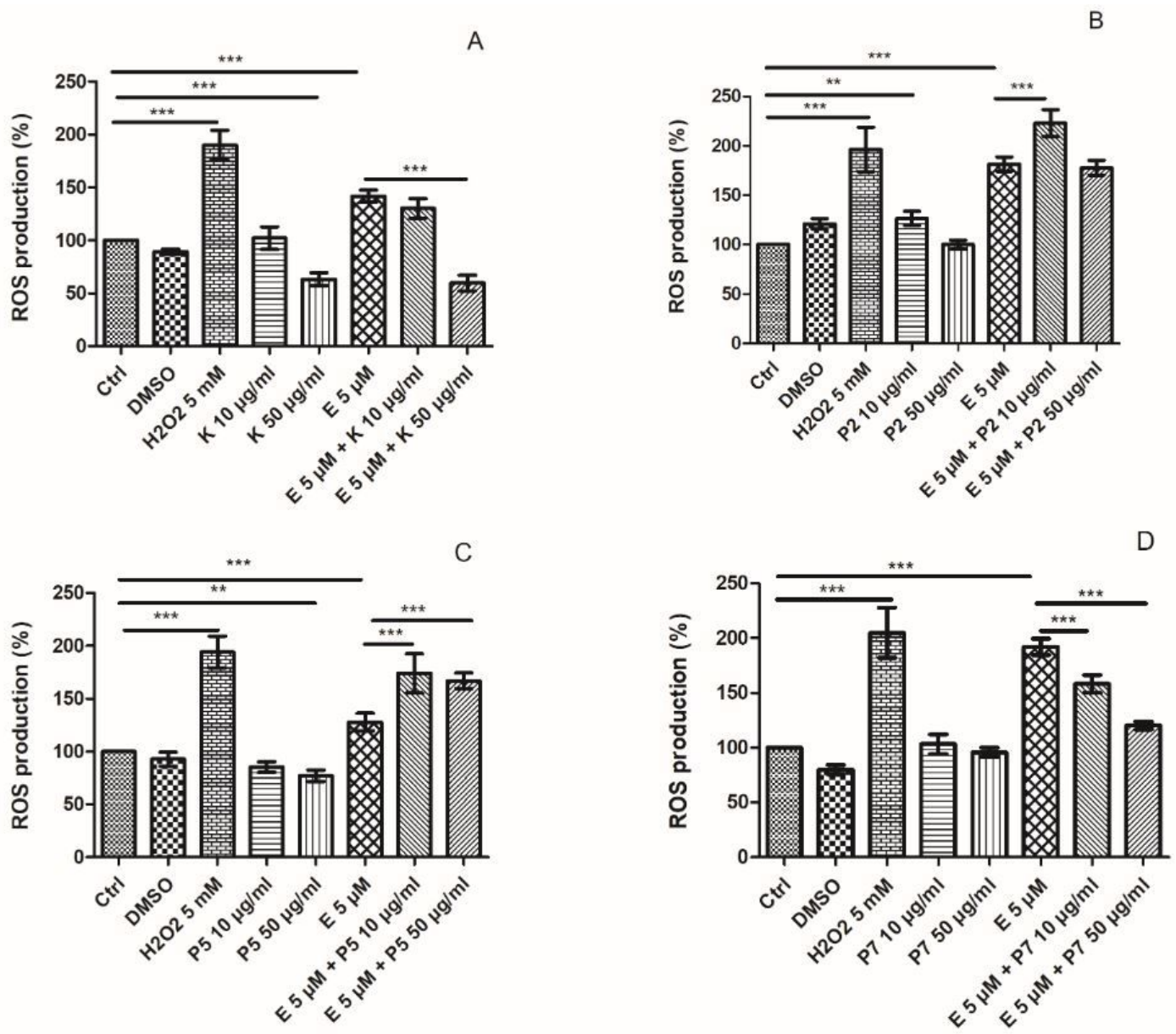


Figure 8

Reactive oxygen species (ROS) level in HL-60 cells incubated for 24 h at 37°C with 5 µM etoposide (E) and 10 µg/ml or 50 µg/ml kaempferol (K) (A), P2 (B), P5 (C) and P7 (D) derivative. The cells incubated with 5 mM H2O2 for 15 min at 37°C were positive control. The figure shows mean results ± SD, n = 6; * p < 0.05, ** p < 0.01, *** p < 0.001.

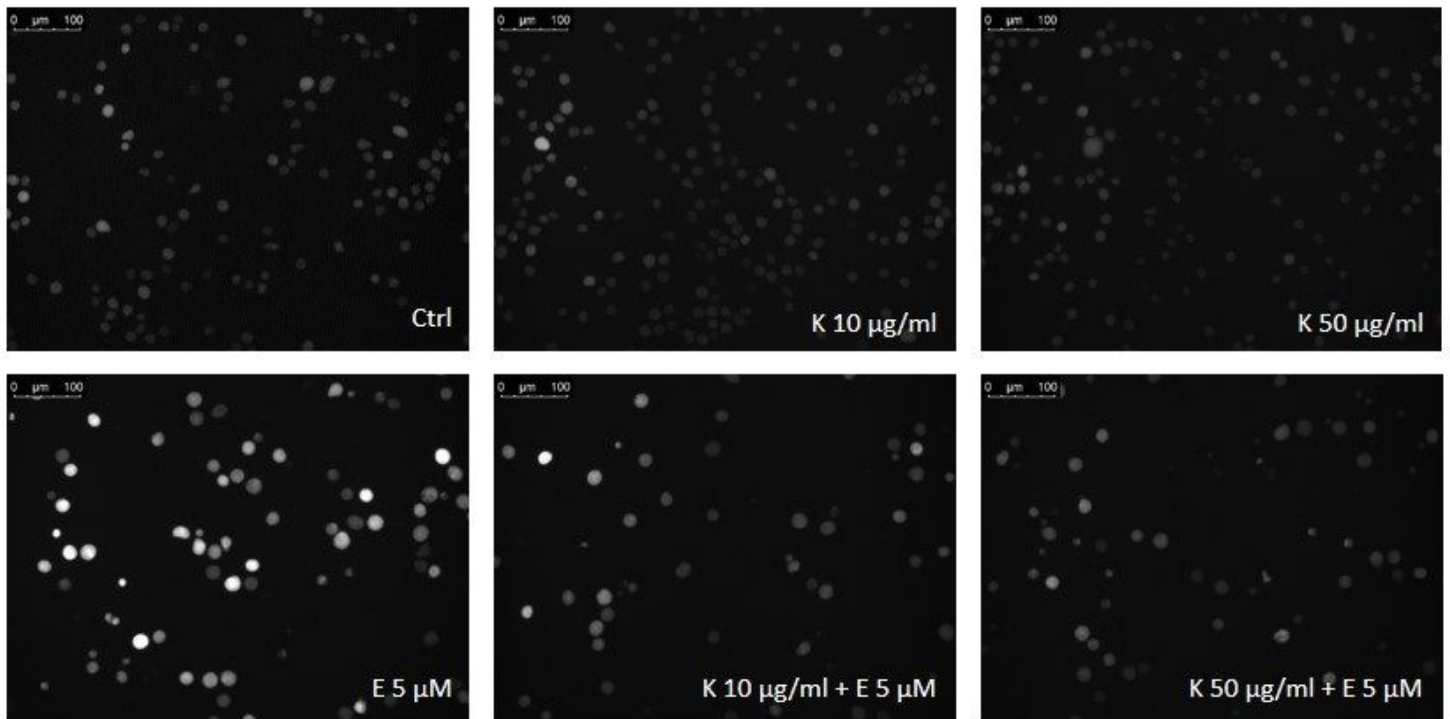


Figure 9

Representative photos of cells with the fluorescence probe H2DCFH-DA after 24 h incubation at 37°C with 5 µM etoposide (E) and 10 µg/ml or 50 µg/ml kaempferol (K). The figure also contains pictures of comets from negative control (Ctrl).

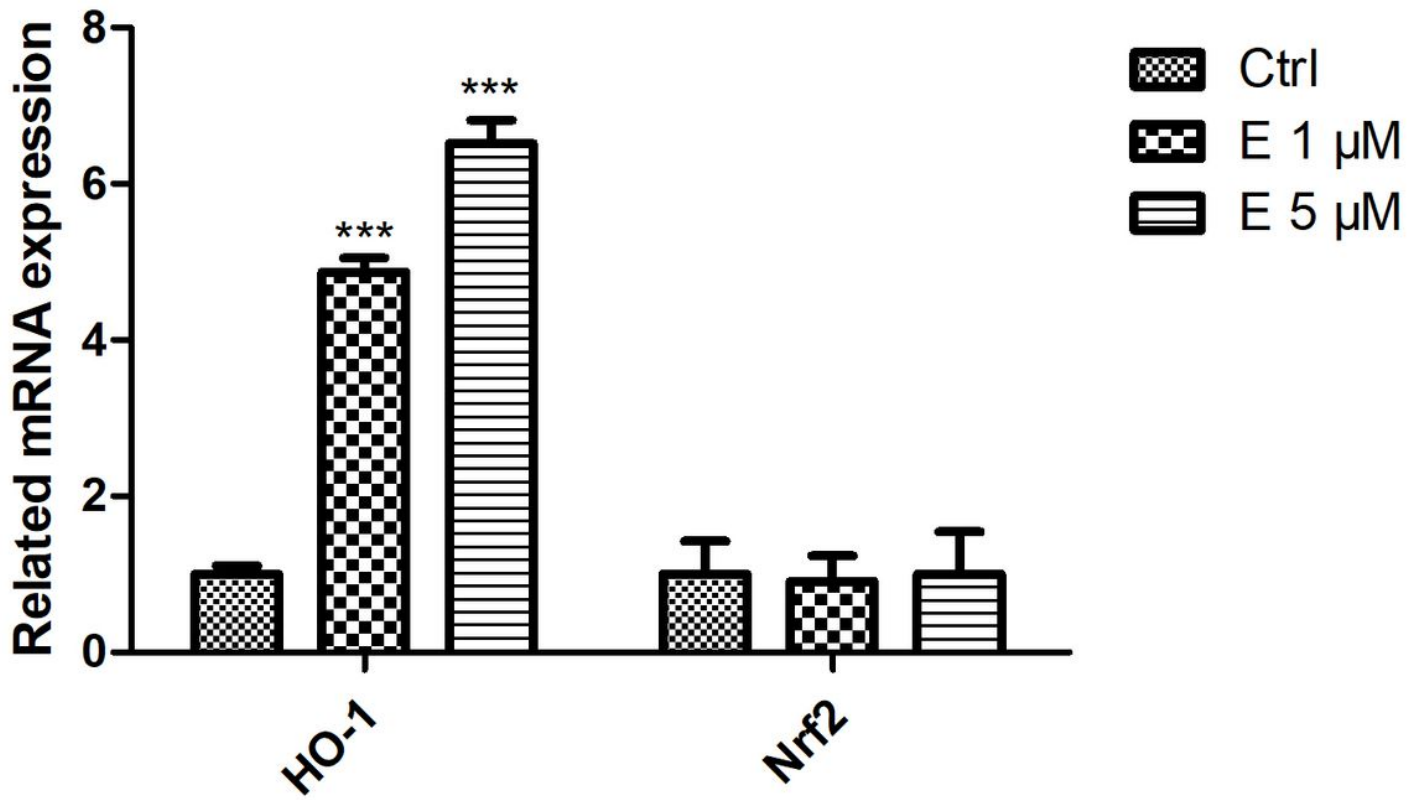


Figure 10

Relative expression of HO-1 and Nrf2 genes in HL-60 cells incubated for 24 h at 37°C with 1 μM or 5 μM etoposide (E). The figure shows mean results \pm SD, n = 4; *** p < 0.001.

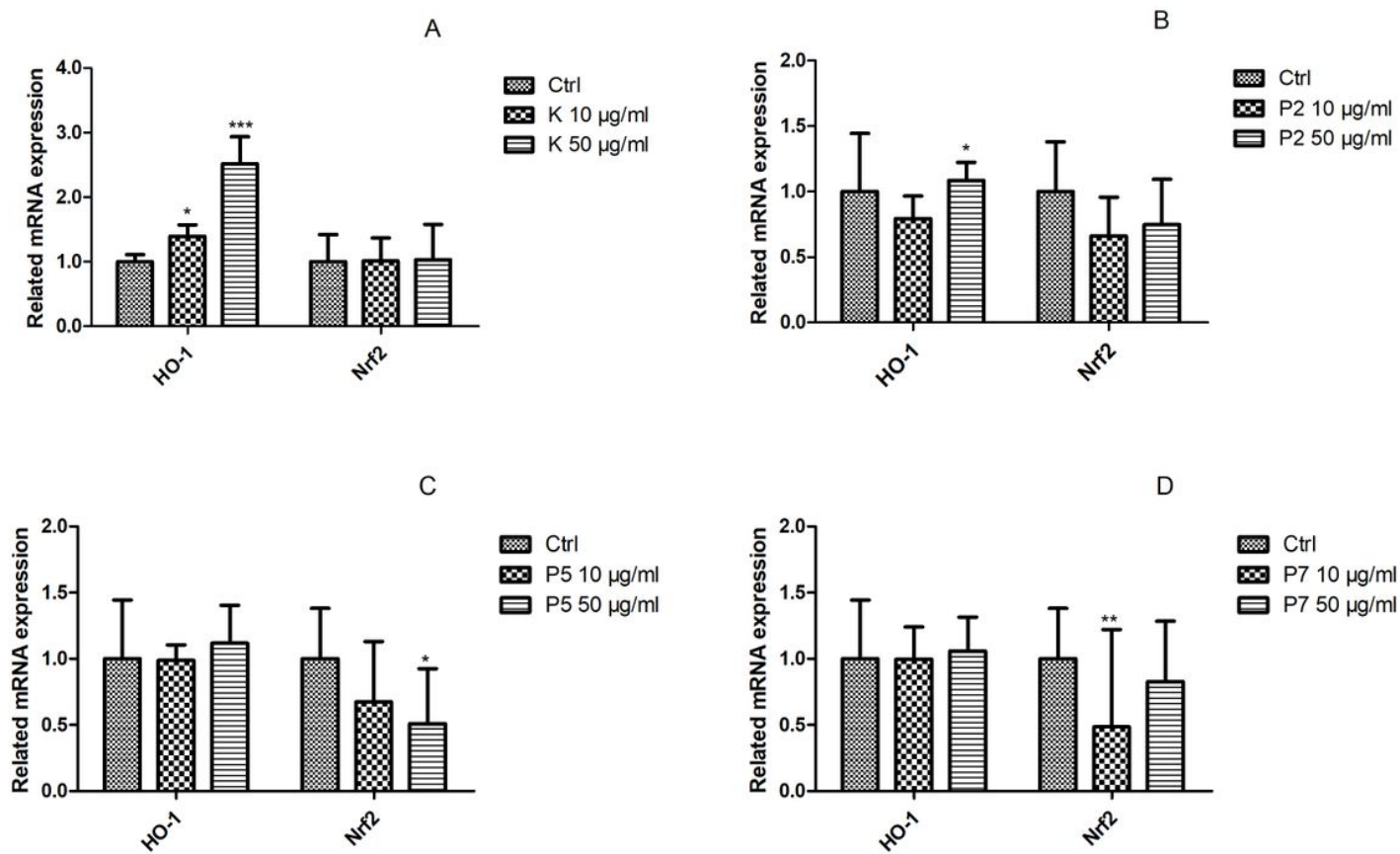


Figure 11

Relative expression of HO-1 and Nrf2 genes in HL-60 cells incubated for 24 h at 37°C with 10 µg/ml or 50 µg/ml kaempferol (K) (A), P2 (B), P5 (C) and P7 (D) derivative. The figure shows mean results \pm SD, n = 4; * p < 0.05, ** p < 0.01, *** p < 0.001.